DECENTRALIZED COORDINATION OF ENERGY RESOURCES IN ELECTRICITY DISTRIBUTION NETWORKS

Nikolaos Gatsis, Likhitha Yalamanchili, Mohammadhafez Bazrafshan, and Paresh Risbud

Dept. of Electrical and Computer Engineering, The University of Texas at San Antonio

ABSTRACT

This paper is concerned with optimal multi-period scheduling of distributed energy resources (DERs) dispersed in electricity distribution networks. DERs considered here comprise programmable loads with the ability to adjust their real power, photovoltaic (PV) generators with the ability to inject or absorb reactive power, as well as storage units (batteries) that can be charged or discharged and also offer the capability of reactive power control. A convex program is formulated to jointly schedule DERs over a time horizon. The objective to be minimized is a weighted combination of energy losses on the lines and cost of power provision offset by end-user satisfaction. A decentralized solver based on the alternating direction method of multipliers (ADMM) is developed, featuring closed-form updates per node and relying only on communication between neighboring nodes.

Index Terms— Distributed algorithms, electricity distribution networks, optimization methods, photovoltaic generators, storage

1. INTRODUCTION

Electricity distribution networks are envisioned to accommodate a variety of devices, ranging from programmable loads and dispersed renewable generation, such as photovoltaic (PV) generators, to electricity storage units (batteries). Programmable loads are instrumental in shaping the rising demand, and renewable generation integrated at distribution networks plays a significant role in meeting future demand using clean energy and bypassing transmission network congestion. Batteries meanwhile offer the capability of storing energy in times of excess generation and returning it in times of energy shortage. Programmable loads, distributed generation, and distributed storage are collectively called *distributed energy resources (DERs)*.

Optimal scheduling of DERs offers opportunities for reliable and economic operation of electricity distribution networks via minimization of network energy losses or power provision costs, and maximization of user satisfaction. Each DER is characterized by different control capabilities. Specifically, the real power consumption of programmable loads can be adjusted, but the corresponding reactive power is determined via the load's power factor. PV units generate power based on solar irradiance, upon which the system designer has no control, but they may also inject or absorb reactive power, which is a decision variable [1]. Last but not least, storage units may be charged or discharged by consuming or delivering real power, and can simultaneously adjust their reactive power [2]. The chief challenge is to come up with scalable algorithms to leverage and coordinate the DER capabilities, in order to achieve network-wide objectives, while respecting the power flow equations.

To addresses the aforementioned challenge, this paper formulates a convex optimization problem to optimally and jointly schedule DERs, and develops a decentralized solver based on the alternating direction method of multipliers (ADMM). Prior work and the contributions of this paper are listed next.

1.1. Relation to prior work and contributions

The development of decentralized algorithms for optimal reactive power compensation from PV units and the coordination with user programmable loads has received wide attention over the last years, see e.g., [1, 3–10] for representative works. Coordination with storage is nevertheless not explored in the aforementioned works. On the other hand, the coupling of storage with renewable energy sources has been previously considered, and offline or online algorithms for optimal storage operation have been developed [11–13]. These works do not account for the physical network; as such, reactive power compensation and voltage specifications are not considered. The impact of storage on transmission networks is the theme of [14] and [15], without considering reactive power compensation by storage or PV units, or developing decentralized solvers.

The first contribution of the paper is to formulate a multi-period optimal scheduling problem for coordination of programmable loads, PV units and batteries, with the latter two providing reactive power compensation. The objective is to minimize system thermal losses and the cost of power import into the distribution system, offset by user satisfaction modeled via utility functions. A linear approximation of the power flow equations, termed simplified DistFlow (see e.g., [6, 16, 17]), is utilized, and the overall problem amounts to a convex quadratically constrained quadratic program (QCQP). The second contribution is to develop a computationally efficient and scalable decentralized solver based on ADMM featuring *closed-form updates* and communication only between *neighboring nodes*. Related decentralization techniques have been reported in [9] and [10], which are extended here to account for storage devices modeled via dynamical equations over a time horizon. Accounting for reactive power from storage necessitates the closed-form solution of a QCQP in 2 variables, which is also derived here.

The remainder of the paper is organized as follows. Section 2 formulates the optimal scheduling problem. Section 3 develops the decentralized solver and outlines the communication requirements. Section 4 provides numerical tests, and Section 5 gives pointers to future directions.

2. PROBLEM FORMULATION

An electricity distribution feeder modeled by a line network is shown in Fig.1. Node 0 represents the substation, while nodes $1, ..., N-$

This material is based upon work supported by the National Science Foundation under Grants CCF-1421583 and ECCS-1462404. This project and the preparation of this study were also funded in part by monies provided by CPS Energy through an Agreement with The University of Texas at San Antonio.

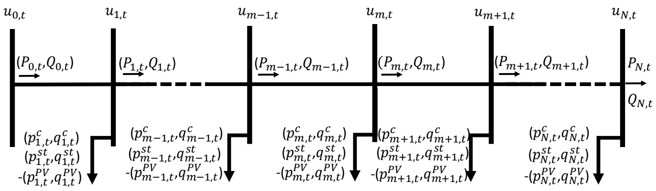

Fig. 1: Line network.

represent the users. Each User $m = 1, ..., N-1$ will have a controllable load, PV generation and a battery to store power generated by PV. The scheduling horizon $S = 1, ..., T$, where each time slot has a duration δ and is generically denoted by t.

2.1. User Load Model

Let $p^c_{m,t}$ and $q^c_{m,t}$ be the real and reactive power consumption at node m at slot t. Let $\mathrm{PF}_m \epsilon (0, 1]$ denote the power factor corresponding to the load of user m. Residential loads operate at constant power factors, and are of inductive nature, that is, $q^c_{m,t} \geq 0$. The reactive power consumption at node m and slot t is related to the real power consumption at node m and slot t via PF_m as follows

$$q^c_{m,t} = p^c_{m,t}\sqrt{1/\mathrm{PF}_m^2 - 1}. \tag{1}$$

The real power consumption $p^c_{m,t}$ is also constrained by lower and upper bounds, i.e.,

$$p^c_{m,t,\min} \leq p^c_{m,t} \leq p^c_{m,t,\max}. \tag{2}$$

2.2. PV Model

Each user m is generically considered to have a PV generation unit; $p^{PV}_{m,t}$ and $q^{PV}_{m,t}$ represents the real and reactive power generated by PV unit at node m and slot t. The quantities $p^{pv}_{m,t}$ will be obtained through a forecast, and hence will be considered given constants in the optimization problem. On the other hand, $q^{pv}_{m,t}$ is a decision variable, and is constrained as follows (see e.g., [1]):

$$|q^{PV}_{m,t}| \leq \sqrt{(S^{PV}_{m,\max})^2 - (p^{PV}_{m,t})^2}. \tag{3}$$

Here, $S^{PV}_{m,max}$ is the maximum apparent power of the PV at node m, and is a hardware-specific constant.

2.3. Storage Model

Each user also has a battery that can be charged or discharged. With $b_{m,t}$ denoting the stored energy in the battery at node m and at the beginning of slot t, the equation modeling the storage dynamics is

$$b_{m,t+1} = b_{m,t} + \delta p^{st}_{m,t}. \tag{4}$$

The variable $p^{st}_{m,t}$ denotes the real power at which the battery is charged or discharged in slot t, depending on whether $p^{st}_{m,t} \geq 0$ or $p^{st}_{m,t} \leq 0$, respectively, and is constrained by charging/discharging limits as follows:

$$-p^{st}_{m,\max} \leq p^{st}_{m,t} \leq p^{st}_{m,\max}. \tag{5}$$

Furthermore, energy storage systems have finite capacity $b_{m,\max}$, which constraints the energy stored at every slot:

$$0 \leq b_{m,t} \leq b_{m,\max}. \tag{6}$$

Note that $b_{m,1}$ is the energy stored at the beginning of slot 1, and is considered known, while $b_{m,T+1}$ is the energy stored at the end of the T-slot scheduling period. The latter could be kept above a given threshold $\bar{b}_m$ (where $0 \leq \bar{b}_m \leq b_{m,\max}$), to achieve reliable and efficient energy scheduling for the next T-slot scheduling period:

$$b_{m,T+1} \geq \bar{b}_m. \tag{7}$$

Storage systems may also have the capability to inject or absorb reactive power, as in the case of PVs [2]. This reactive power is denoted by $q^{st}_{m,t}$, and is constrained in a fashion similar to (3) by

$$(p^{st}_{m,t})^2 + (q^{st}_{m,t})^2 \leq (S^{st}_{m,\max})^2 \tag{8}$$

where $S^{st}_{m,\max}$ is the maximum apparent power capability by the battery. Note that while (3) becomes a linear constraint, (8) is a (convex) quadratic constraint.

2.4. Power Flows

As the real and reactive power generation or consumption of PV changes from user to user at each time period, the power flows in the distribution network will also be time dependent. Let $P_{m,t}$ and $Q_{m,t}$ be the real and reactive power flows from node m to $m+1$ at slot t; and $u_{m,t}$ be the squared magnitude of voltage phasor at node m at slot t. The power flows at the lines, the nodal voltages, and the nodal power injections are related via the power flow equations which are in general nonconvex. A convex approximation called simplified DistFlow is used in this paper as follows:

$$P_{m+1,t} = P_{m,t} - (p^{st}_{m+1,t} + p^c_{m+1,t} - p^{PV}_{m+1,t}) \tag{9a}$$

$$Q_{m+1,t} = Q_{m,t} - (q^c_{m+1,t} - q^{PV}_{m+1,t} - q^{st}_{m+1,t}) \tag{9b}$$

$$u_{m+1,t} = u_{m,t} - 2(r_m P_{m,t} + x_m Q_{m,t}) \tag{9c}$$

where $t = 1, \ldots, T$, $m = 0, \ldots, N-1$, with the conditions

$$P_{N,t} = 0,\ Q_{N,t} = 0,\ u_{0,t} = V_0^2. \tag{10}$$

The real and reactive power exiting node N is zero because N is the last node in the network, while V_0 is the constant voltage magnitude at the substation. Also, r_m and x_m are respectively the resistance and reactance of the line connecting nodes m and $m+1$.

2.5. Objective Function

The objective function to be minimized has three parts: 1) the cost of the real power imported in the distribution system, 2) negative of the user utility function, and 3) the thermal losses over the network.

Specifically, the cost of the real power to operate the distribution system is given by $a_t P_{0,t}$ where a_t is the price of one unit of power, and $P_{0,t}$ is the power flowing from substation into the network. Prices $(a_t)_{t=1}^T$ are known in advance of the horizon; note also that $P_{0,t}$ can be positive or negative. In addition, a utility function of $p^c_{m,t}$ is introduced in order to account for the end-user satisfaction. While any concave utility function could be used, a linear form $K_{m,t}p^c_{m,t}$ is adopted here, where the coefficient is allowed to vary with time. Finally, the thermal losses on the lines of the network in the adopted power flow model can be approximated by the term $\sum_m (P^2_{m,t} + Q^2_{m,t})/V_0^2$. Putting everything together, the optimal DER scheduling problem is a convex QCQP expressed as

$$\min \sum_{t=1}^{T} a_t P_{0,t} - \sum_{m=1}^{N}\sum_{t=1}^{T} K_{m,t}p^c_{m,t} + \sum_{m=0}^{N-1}\sum_{t=1}^{T} r_m\left(\frac{P^2_{m,t} + Q^2_{m,t}}{V_0^2}\right) \tag{11}$$

subject to (1)–(10).

Objective component weights can be absorbed in a_t and $K_{m,t}$.

3. DECENTRALIZED ALGORITHM

In this section, a decentralized solver for (11) based on ADMM is developed. Recall that ADMM requires writing the optimization problem as $\min f(\mathbf{x}) + g(\mathbf{z})$ subject to a coupling constraint $\mathbf{A}\mathbf{x} + \mathbf{B}\mathbf{z} = \mathbf{c}$ and possibly individual constraints for $\mathbf{x}$ and $\mathbf{z}$ [18]. Properly designed auxiliary variables need to be introduced in order to write (11) in the aforementioned form, and simultaneously enable closed-form per node updates. This task is undertaken in the ensuing subsection. Subsection 3.2 briefly describes the closed-form updates, and Subsection 3.3 outlines the required neighbor-to-neighbor communication for algorithm implementation.

3.1. Equivalent problem

Auxiliary variables annotated with tilde or hat are introduced in the following problem, which is easily seen to be equivalent to (11) thanks to the coupling constraints.

$$\min \sum_{t=1}^{T} a_t P_{0,t} - \sum_{m=1}^{N}\sum_{t=1}^{T} K_{m,t}(\tilde{p^c}_{m,t}) + \sum_{m=0}^{N-1}\sum_{t=1}^{T} r_m \frac{P_{m,t}^2 + Q_{m,t}^2}{V_0^2} \tag{12a}$$

subject to
Coupling Constraints

$$m = 0, ..., N-1, \;\; t = 1, ..., T \begin{cases} \tilde{P}_{m,t} = P_{m,t} \\ \tilde{P}_{m,t} = \hat{P}_{m,t} \\ \tilde{Q}_{m,t} = Q_{m,t} \\ \tilde{Q}_{m,t} = \hat{Q}_{m,t} \end{cases} \tag{12b}$$

$$m = 1, ..., N, \;\; t = 1, ..., T \begin{cases} \tilde{u}_{m,t} = u_{m,t} \\ \tilde{u}_{m,t} = \hat{u}_{m,t} \end{cases} \tag{12c}$$

$$m = 1, ..., N, \;\; t = 1, ..., T \begin{cases} \tilde{p^c}_{m,t} = p^c_{m,t} \\ \tilde{p}^{st}_{m,t} = p^{st}_{m,t} \\ \tilde{q}^{st}_{m,t} = q^{st}_{m,t} \\ \tilde{q}^{PV}_{m,t} = q^{PV}_{m,t} \end{cases} \tag{12d}$$

$$\tilde{b}_{m,t} = b_{m,t} \;\text{ for }\; m = 1, ..., N, \;\; t = 2, ..., T+1 \tag{12e}$$

Individual Constraints

$$P_{m,t} = \hat{P}_{m-1,t} - (p^{st}_{m,t} + p^c_{m,t} - p^{PV}_{m,t}) \tag{12f}$$

$$Q_{m,t} = \hat{Q}_{m-1,t} - (p^c_{m,t}\sqrt{\frac{1}{\mathrm{PF}^2} - 1} - q^{PV}_{m,t} - q^{st}_{m,t}) \tag{12g}$$

$$\hat{u}_{m+1,t} = u_{m,t} - 2(r_m P_{m,t} + x_m Q_{m,t}) \tag{12h}$$

$$b_{m,t+1} = b_{m,t} + \delta p^{st}_{m,t} \tag{12i}$$

$$|\tilde{q}^{PV}_{m,t}| \leq \sqrt{(S^{PV}_{m,max})^2 - (p^{PV}_{m,t})^2} \tag{12j}$$

$$(\tilde{p}^{st}_{m,t})^2 + (\tilde{q}^{st}_{m,t})^2 \leq (S^{st}_{m,max})^2 \tag{12k}$$

$$(1-\epsilon)^2 V_0^2 \leq \tilde{u}_{m,t} \leq (1+\epsilon)^2 V_0^2 \tag{12l}$$

$$0 \leq \tilde{b}_{m,t} \leq b_{m,max} \tag{12m}$$

$$-p^{st}_{m,max} \leq \tilde{p}^{st}_{m,t} \leq p^{st}_{m,max} \tag{12n}$$

$$\bar{b}_m \leq \tilde{b}_{m,T+1} \leq b_{m,max} \tag{12o}$$

$$p^c_{m,t,min} \leq \tilde{p}^c_{m,t} \leq p^c_{m,t,max} \tag{12p}$$

Table 1: Coupling Constraints and Associated Lagrange Multipliers

$\tilde{P}_{m,t} = P_{m,t}$	$\tilde{P}_{m,t} = \hat{P}_{m,t}$	$\tilde{Q}_{m,t} = Q_{m,t}$	$\tilde{Q}_{m,t} = \hat{Q}_{m,t}$
$\lambda_{m,t}$	$\hat{\lambda}_{m,t}$	$\mu_{m,t}$	$\hat{\mu}_{m,t}$
$\tilde{u}_{m,t} = u_{m,t}$	$\tilde{u}_{m,t} = \hat{u}_{m,t}$	$\tilde{p}^c_{m,t} = p^c_{m,t}$	$\tilde{p}^{st}_{m,t} = p^{st}_{m,t}$
$\gamma_{m,t}$	$\hat{\gamma}_{m,t}$	$\omega_{m,t}$	$\hat{\eta}_{m,t}$
$\tilde{q}^{st}_{m,t} = q^{st}_{m,t}$	$\tilde{q}^{PV}_{m,t} = q^{PV}_{m,t}$	$\tilde{b}_{m,t} = b_{m,t}$	
$\nu_{m,t}$	$\theta_{m,t}$	$\zeta_{m,t}$	

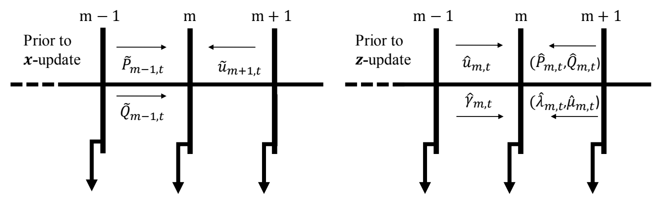

Fig. 2: Communication requirements per iteration of ADMM solver

The optimization variables of the previous problem are organized into vectors $\mathbf{x}_m$ and $\mathbf{z}_m$, corresponding to nodes $m = 0, 1, \ldots, N$. Variable $\mathbf{x}_m$ includes $P_{m,t}$, $Q_{m,t}$, $u_{m,t}$, $\hat{P}_{m-1,t}$, $\hat{Q}_{m-1,t}$, $\hat{u}_{m+1,t}$, $p^c_{m,t}$, $q^{PV}_{m,t}$, $p^{st}_{m,t}$, $q^{st}_{m,t}$, $b_{m,t}$ for all t; while $\mathbf{z}_m$ collects $\tilde{p}^c_{m,t}, \tilde{q}^{PV}_{m,t}, \tilde{p}^{st}_{m,t}, \tilde{q}^{st}_{m,t}, \tilde{b}_{m,t}$ for all t. Upon defining the equivalent problem, Lagrange multipliers are assigned to coupling constraints as listed in Table 1, and then the augmented Lagrangian function can be formed, which is not shown here for brevity.

3.2. Closed-form updates

The ADMM updates proceed with minimization with respect to $\mathbf{x}$ keeping $\mathbf{z}$ constant, and vice versa. Writing out the augmented Lagrangian function, it is not hard to see that the update for $\mathbf{x}_m$ amounts to a quadratic program subject to linear equality constraints, which has a a well-known closed-form solution (see e.g., [10]).

The $\mathbf{z}_m$-update breaks down into two types of updates. Firstly, the update for each of $\tilde{P}_{m,t}, \tilde{Q}_{m,t}, \tilde{u}_{m,t}, \tilde{p}^c_{m,t}, \tilde{q}^{PV}_{m,t}, \tilde{b}_{m,t}$ becomes a quadratic program in a *single* variable, possibly with a lower and upper bound, and thus also has a closed-form solution.

Secondly, the update for $\tilde{p}^{st}_{m,t}$ and $\tilde{q}^{st}_{m,t}$ is a QCQP in two variables, which is stated as follows.

$$\min_{\tilde{p}_{m,t}, \tilde{q}_{m,t}} \; \frac{\rho}{2}(\tilde{p}^{st}_{m,t})^2 + \frac{\rho}{2}(\tilde{q}^{st}_{m,t})^2 - \tilde{p}^{st}_{m,t}(\rho p^{st}_{m,t} + \eta_{m,t}) - \tilde{q}^{st}_{m,t}(\rho q^{st}_{m,t} + \nu_{m,t}) \tag{13a}$$

subject to:

$$(\tilde{p}^{st}_{m,t})^2 + (\tilde{q}^{st}_{m,t})^2 \leq (S^{st}_{m,max})^2 \tag{13b}$$

$$-p^{st}_{m,max} \leq \tilde{p}^{st}_{m,t} \leq p^{st}_{m,max}. \tag{13c}$$

In order to come up with the solution of the previous problem, let κ be the Lagrange multiplier for (13b); $\bar{\kappa}, \underline{\kappa}$ for (13c). The KKT conditions for problem (13) amount to the following system of equations in variables $(\tilde{p}^{st}_{m,t}, \tilde{q}^{st}_{m,t}, \kappa, \bar{\kappa}, \underline{\kappa})$:

$$(\rho + 2\kappa)\tilde{p}^{st}_{m,t} + \bar{\kappa} - \underline{\kappa} = \rho p^{st}_{m,t} + \eta \tag{14a}$$

$$(\rho + 2\kappa)\tilde{q}^{st}_{m,t} = \rho q^{st}_{m,t} + \nu \tag{14b}$$

$$\kappa[(\tilde{p}^{st}_{m,t})^2 + (\tilde{q}^{st}_{m,t})^2 - (S^{st}_{m,max})^2] = 0 \tag{14c}$$

$$\bar{\kappa}(-p^{st}_{m,max} + \tilde{p}^{st}_{m,t}) = 0 \tag{14d}$$

$$\underline{\kappa}(-p^{st}_{m,max} - \tilde{p}^{st}_{m,t}) = 0. \tag{14e}$$

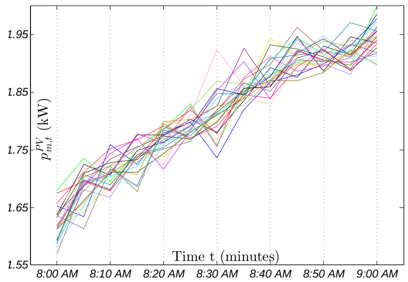

Fig. 3: User PV profiles $p^{PV}_{m,t}$ for all m.

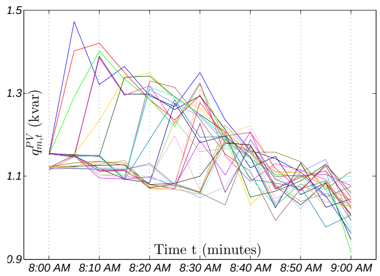

Fig. 4: PV-provided reactive power $q^{PV}_{m,t}$ for all m.

The optimal solution of (13) is obtained by enumerating the eight possible combinations of $\kappa, \bar{\kappa}, \underline{\kappa}$ being zero or not. For example, if $\kappa, \bar{\kappa}, \underline{\kappa}$ are all zero, the corresponding solution can be found from (14a) and (14b) for $\tilde{p}^{st}_{m,t}$ and $\tilde{q}^{st}_{m,t}$. If $\kappa \neq 0$ and $\bar{\kappa}, \underline{\kappa}$ are zeros, the corresponding solution can be found by using (14c). Among the eight corresponding solutions, the one that has the least objective value will be the optimal $\tilde{p}^{st}_{m,t}$ and $\tilde{q}^{st}_{m,t}$.

3.3. Communication requirements

Node m is responsible for maintaining and updating $\mathbf{x}_m$, $\mathbf{z}_m$, and the Lagrange multipliers indexed by m. Fig. 2 shows the communication requirements to this end. Prior to $\mathbf{x}_m$-update, node m receives $\tilde{P}_{m-1,t}$ and $\tilde{Q}_{m-1,t}$ from node $m-1$; and $\tilde{u}_{m+1,t}$ from node $m+1$. Likewise, prior to $\mathbf{z}_m$-update, node m receives $\hat{P}_{m,t}$ and $\hat{Q}_{m,t}$ from node $m+1$; and $\hat{u}_{m,t}$ from node $m-1$. Fig. 2 also depicts the required exchange of Lagrange multipliers. Due to the closed-form per-node updates and the communication between neighboring nodes, the developed solver is computationally efficient and scalable.

4. NUMERICAL TESTS

Numerical tests are performed on a radial distribution network with $N = 25$ nodes. The substation voltage is fixed at 7.2 kV, and the line resistance and reactance values are $0.066\ \Omega$ and $0.076\ \Omega$, respectively. The maximum voltage deviation per node is set to $\epsilon = 0.03$.

The NREL Solar Power Data for Integration Studies from April 2006 4^{th} are used to generate the PV profile [19]. The time horizon extends from 8:00 AM until 9:00 AM with time step $\delta = 5$ minutes, which corresponds to $T = 13$ as the length of the time horizon. The profile of PV injections $\{p^{PV}_{m,t}\}_{m=1}^{M}$ for all t is generated as a Gaussian random vector with mean specified by the NREL data and covariance matrix $\mathbf{C}$ with exponentially decreasing entries $\mathbf{C}_{ij} = e^{-0.5|i-j|}$ to model spatial correlation; see e.g., [20] for a related model. The resulting profiles are scaled so that the peak PV generation is 2 kW, and are depicted in Fig. 3.

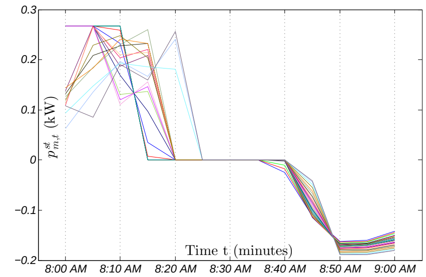

Fig. 5: Battery charge and discharge profiles $p^{st}_{m,t}$ for all m.

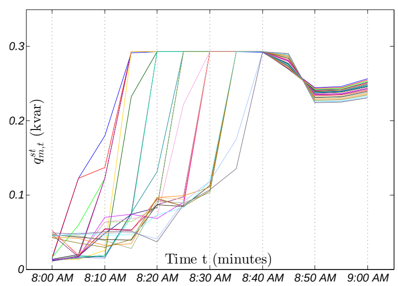

Fig. 6: Battery-provided reactive power $q^{st}_{m,t}$ for all m.

The maximum apparent power capacity of the PV inverter is selected to be $S^{PV}_{m,max} = 2.2$ kVA. The storage capacity is set to $b_{m,\max} = 4$ kWh while the minimum energy stored required at the beginning of the next horizon is $\bar{b}_m = 0.25\, b_{m,\max}$ for all m. The maximum real power that can be generated or consumed in the battery is $p^{st}_{m,\max} = 0.26$ kW. The interval for user real and reactive power consumption is $[p^c_{m,t,\min}, p^c_{m,t,\max}] = [4\text{ kW}, 6\text{ kW}]$, while the user utility function coefficient $K_{m,t}$ is increasing linearly from 0.001 to 0.005 across t for all m.

The optimal reactive power provided by the PV units is given in Fig. 4. Fig. 5 depicts the battery charge and discharge profiles, while the battery-provided reactive power is illustrated in Fig. 6. The linear increase of $K_{m,t}$ here implies that the user load is increasing across time. The optimal schedule entails initially charging the battery, and then discharging it, as illustrated in Fig. 5, in order to compensate for the increased demand towards the end of the horizon and simultaneously satisfy the terminal constraint for the storage [cf. (7)].

Fig. 4 reveals that as time evolves (and the user load increases), more PV units provide reactive power support. But as the PV generation ramps up at the end of the horizon, the capability of the PV units to provide reactive power decreases [cf. (3)], and additional reactive power is injected by the storage units, as depicted in Fig. 6.

5. FUTURE DIRECTIONS

This work can be expanded along several avenues. First, the uncertainty in PV generation can be accounted for, as opposed to relying on forecasts here. Another direction is the incorporation of tree networks, which constitute a generalization of the line network as a model for electricity distribution systems. It is also worth investigating the multi-period optimal scheduling problem with the second-order cone relaxation of the power flow equations, which is a more accurate model than the linear power flows adopted here.

6. REFERENCES

[1] K. Turitsyn, P. Šulc, S. Backhaus, and M. Chertkov, “Options for control of reactive power by distributed photovoltaic generators,” *Proc. of the IEEE*, vol. 99, no. 1, pp. 1063–1073, June 2011.

[2] Mostafa Nick, Rachid Cherkaoui, and Mario Paolone, “Optimal allocation of dispersed energy storage systems in active distribution networks for energy and grid support,” *IEEE Trans. Power Syst.*, vol. 29, no. 5, pp. 2300–2310, Sept. 2014.

[3] N. Li, L. Chen, and S. H. Low, “Demand response in radial distribution networks: Distributed algorithm,” in *Proc. Asilomar Conf. Signals, Systems, and Computers*, Pacific Grove, CA, Nov. 2012, pp. 1549–1553.

[4] A. Lam, B. Zhang, A. Dominguez-Garcia, and D. Tse, “Optimal distributed voltage regulation in power distribution networks,” *arxiv*, Apr. 2012.

[5] S. Bolognani, R. Carli, G. Cavraro, and S. Zampieri, “A distributed control strategy for optimal reactive power flow with power and voltage constraints,” in *Proc. 52nd IEEE Conf. Decision and Control*, Firenze, Oct. 2013, pp. 115–120.

[6] P. Šulc, S. Backhaus, and M. Chertkov, “Optimal distributed control of reactive power via the alternating direction method of multipliers,” *IEEE Trans. Energy Convers.*, vol. 29, no. 4, pp. 968–977, Dec. 2014.

[7] E. Dall’Anese, S. Dhople, B. Johnson, and G. B. Giannakis, “Decentralized optimal dispatch of photovoltaic inverters in residential distribution systems,” *IEEE Trans. Energy Convers.*, vol. 29, no. 4, pp. 957–967, Dec. 2014.

[8] E. Dall’Anese, H. Zhu, and G. B. Giannakis, “Distributed optimal power flow for smart microgrids,” *IEEE Trans. Smart Grid*, vol. 4, no. 3, pp. 1464–1475, Sept. 2013.

[9] Q. Peng and S. H. Low, “Distributed algorithm for optimal power flow on a radial network,” *arxiv*, May. 2015.

[10] M. Bazrafshan and N. Gatsis, “Decentralized stochastic programming for real and reactive power management in distribution systems,” in *Proc. IEEE Int. Conf. Smart Grid Communications*, Venice, Italy, Nov. 2014, pp. 218–223.

[11] S. Lakshminarayana, T.Q.S. Quek, and H.V. Poor, “Cooperation and storage tradeoffs in power grids with renewable energy resources,” *IEEE J. Sel. Areas Commun.*, vol. 32, no. 7, pp. 1386–1397, July 2014.

[12] K. Rahbar, J. Xu, and R. Zhang, “Real-time energy storage management for renewable integration in microgrid: An off-line optimization approach,” *IEEE Trans. on Smart Grid*, vol. 6, no. 1, pp. 124–134, Jan. 2015.

[13] S. Sun, M. Dong, and B. Liang, “Distributed real-time power balancing in renewable-integrated power grids with storage and flexible loads,” *IEEE Trans. Smart Grid*, 2015, to appear (available at IEEE Early Access).

[14] D. Gayme and U. Topcu, “Optimal power flow with distributed energy storage dynamics,” in *Proc. American Control Conference*, June 2011, pp. 1536–1542.

[15] A. J. Lamadrid, “Optimal use of energy storage systems with renewable energy sources,” *International Journal of Electrical Power & Energy Systems*, vol. 71, pp. 101–111, 2015.

[16] M. E. Baran and F. F. Wu, “Optimal sizing of capacitors placed on a radial distribution feeder,” *IEEE Trans. Power Del.*, vol. 4, no. 1, pp. 735–743, Jan. 1989.

[17] M. E. Baran and F. F. Wu, “Network reconfiguration in distribution systems for loss reduction and load balancing,” *IEEE Trans. Power Del.*, vol. 4, no. 2, pp. 1401–1407, Apr. 1989.

[18] S. Boyd, N. Parikh, E. Chu, B. Peleato, and J. Eckstein, “Distributed optimization and statistical learning via the alternating direction method of multipliers,” *Foundations and Trends in Machine Learning*, vol. 3, no. 1, pp. 1–122, 2011.

[19] National Renewable Energy Labaratory, “Solar power data for integration studies,” [Online.] Available: http://www.nrel.gov/electricity/transmission/solar_integration_methodology.html.

[20] E. Dall’Anese, S. V. Dhople, B. B. Johnson, and G. B. Giannakis, “Optimal dispatch of residential photovoltaic inverters under forecasting uncertainties,” *IEEE J. Photovolt.*, vol. 5, no. 1, pp. 350–359, Jan. 2015.